ORIGINAL RESEARCH

Prospective Follow-Up of Cortical Interruptions, Bone Density, and Micro-structure Detected on HR-pQCT: A Study in Patients with Rheumatoid Arthritis and Healthy Subjects

M. Peters[1,2,3] · J. P. van den Bergh[1,3,7,8] · P. Geusens[1,2,7] · A. Scharmga[1,2,3] · D. Loeffen[4] · R. Weijers[4] · B. van Rietbergen[5,6] · A. van Tubergen[1,2]

Abstract

Objectives The purpose of the study was to prospectively investigate change (repair or progression) in the number, surface area and volume of cortical interruptions, bone density (vBMD) and micro-structural parameters assessed by high-resolution peripheral quantitative computed tomography (HR-pQCT) in finger joints of patients with rheumatoid arthritis (RA) treated with synthetic disease modifying anti-rheumatic drugs (sDMARDs) and/or biologic DMARDs (bDMARDs) over a 1-year follow-up period, and in comparison with healthy subjects (HS).

Methods Thirty-two patients with RA (221 joints, 53% on bDMARDs) and 32 HS (117 joints) were assessed at baseline and after 1 year using semi-automatic analysis of HR-pQCT images. Mean changes (group level) and the proportion of joints (joint level) with changes beyond the least significant change were calculated.

Results At baseline, 530 interruptions were identified in patients, and 136 in HS. The mean of the interruption parameters did not significantly change in either group Mean vBMD decreased more in patients than in HS (-4.4 versus -1.1 mgHA/cm^3, respectively). In patients versus HS, proportionally more joints showed repair in interruption volume (6.6% versus 1.7%, respectively) and loss of vBMD (26.7% versus 12.9%, respectively). In patients on sDMARDs versus patients on bDMARDs, proportionally more joints showed progression in the number of interruptions and loss of vBMD (6.1% versus 1.8% and 31.3% versus 17.2%, respectively).

Conclusions HR-pQCT is able to quantify bone repair and progression. Cortical interruption-, vBMD-, and micro-structure were impaired in RA, of which vBMD and micro-structure further deteriorated, particularly in patients on sDMARDs.

Keywords Cortical interruptions · Rheumatoid arthritis · High-resolution peripheral quantitative computed tomography · Bone mineral density · Disease modifying anti-rheumatic drugs

✉ M. Peters
michiel.peters@maastrichtuniversity.nl

1 Division of Rheumatology, Department of Internal Medicine, Maastricht University Medical Center, P.O. Box 5800, NL-6202 AZ Maastricht, The Netherlands

2 Research School CAPHRI, School for Public Health and Primary Care, Maastricht, The Netherlands

3 NUTRIM School of Nutrition & Translational Research in Metabolism, Maastricht University, Maastricht, The Netherlands

4 Department of Radiology, Maastricht University Medical Center, Maastricht, The Netherlands

5 Faculty of Biomedical Engineering, Eindhoven University of Technology, Eindhoven, The Netherlands

6 Department of Orthopaedic Surgery, Maastricht University Medical Center, Maastricht, The Netherlands

7 Faculty of Medicine and Life Sciences, Hasselt University, Hasselt, Belgium

8 Department of Internal Medicine, VieCuri Medical Center, Venlo, The Netherlands

Introduction

In rheumatoid arthritis (RA), increased osteoclast activity by disease-specific auto-antibodies and pro-inflammatory cytokines can result in peri-articular bone erosions (i.e., pathological cortical interruptions), loss of bone density, and micro-structure [1, 2].

High-resolution peripheral quantitative computed tomography (HR-pQCT) allows in vivo evaluation of the three-dimensional (3D) bone micro-structure with an isotropic voxel size of 82 μm. It has a higher sensitivity to detect erosions than conventional radiography (CR), magnetic resonance imaging (MRI), and computed tomography (CT) [3, 4], and enables to evaluate small cortical interruptions, the volumetric bone mineral density (vBMD), and bone micro-structure in finger joints [5–7]. Studies with HR-pQCT showed not only more and larger cortical interruptions, but also an impaired vBMD and micro-structure in patients with RA, with and without visible erosions on CR, compared with healthy subjects (HS) [7]. Moreover, HR-pQCT demonstrated promising results in evaluating progressive damage and repair processes in patients with RA [8–12]. Repair of bone was primarily found in patients treated with biological disease modifying anti-rheumatic drugs (bDMARDs) [8–11]. However, these studies mainly focused on the presence and change in size of large, pathological interruptions. Changes in small cortical interruptions and micro-structural parameters have not been examined, nor were any comparisons made to a healthy population, in which cortical interruptions can also be found [13]. Although small interruptions might not be specific for RA [13], they might be prone to bone resorption early in the course of RA and can therefore be the first sign of an erosion [1].

Recently, we developed a semi-automatic algorithm that reliably detects the number, surface area, and volume of small cortical interruptions (diameter ≥ 0.41 mm) and validated detection of these interruptions to microCT, the 3D gold standard [5, 14] In the present study, we prospectively investigate change in number, surface area, and volume of cortical interruptions, vBMD- and micro-structural parameters in patients with RA (treated with sDMARDs and/or bDMARDs) with a 1-year follow-up period, and compared our results with a population of HS. We analyzed the results at the group level and at the individual joint level.

We hypothesized that the semi-automatic HR-pQCT image analysis was able to quantify differences within patients with RA, between patients with RA and HS, and between patients treated with sDMARDS and bDMARDs with respect to change in number, surface area, and volume of cortical interruptions, vBMD and micro-structure in finger joints after 1 year.

Materials and Methods

Design and Subjects

For this longitudinal study, we used data from the MOSA-Hand cohort, which consists of 38 healthy female subjects and 41 female patients with RA [6]. They were recruited at the Maastricht University Medical Center, the Netherlands. All patients fulfilled the 2010 American College of Rheumatology (ACR)/European League Against Rheumatism (EULAR) classification criteria for RA [15]. Disease duration, medication use, smoking status, erythrocyte sedimentation rate (ESR), health assessment questionnaire (HAQ) [16], anti-citrullinated protein antibody, and rheumatoid factor positivity were retrieved from the patients' medical file. HS, matched on age by decade, had not suffered from hand joint complaints.

CR Acquisition and Scoring

Posterior-anterior radiographs of the hands were taken from all subjects according to a standard clinical protocol at baseline. Two experienced and trained rheumatologists independently scored the radiographs of the hands in order to assess bone damage according to the Sharp/Van der Heijde (SvdH) method [17]. Mean scores of the two readers were calculated and used for the analysis.

Joints with an SvdH erosion score > 0 in the second and third MCP and PIP joints were excluded from further analysis, because we were specifically interested in small cortical interruptions not visible on CR.

HR-pQCT Image Acquisition

Second and third MCP and PIP joints were scanned at baseline and 1 year later with HR-pQCT (XtremeCT1, Scanco Medical AG, Switzerland) according to the HR-pQCT imaging protocol proposed by The Study group for xtrEme Computed Tomography in RA (SPECTRA), since these joints are most prone for the development of erosions [18, 19]. In patients with RA, both hands were scanned and in HS only the dominant hand as per request of the ethical committee. The hands were scanned using a carbon cast for finger scanning as provided by the manufacturer.

Scanning was performed at clinical in vivo settings, i.e., at 60kVp tube voltage, 900 μA tube current, 100 ms integration time, and images were reconstructed using an 82 μm isotropic voxel size. Scans were graded for motion artifacts according to Pialat et al. [20]. Scans with at least one stack of poor quality (grade > 3) were excluded from further analyses.

HR-pQCT Image Analyses

The outer margin of the cortex was identified using an auto-contouring algorithm [5]. The contours were visually inspected and, if necessary, corrected by an operator as described elsewhere [21]. A segmentation to distinguish bone and non-bone was performed using the standard evaluation protocol from the manufacturer, which included Laplace-Hamming filtering and thresholding [22]. The default area matching algorithm was used to cross-sectionally match baseline and follow-up scan areas, after which the common region was analyzed.

Cortical Interruptions

An automated algorithm for the detection of cortical interruptions and underlying trabecular bone void was applied to all binary images and is described in previous work [5, 14]. In short, first, a cortical mask with a constant thickness of 4 voxels (0.328 mm) was generated based on the outer contour. Second, the bone within this mask was analyzed for discontinuities that can be considered cortical interruptions (≥ 0.41 mm) [14]. Third, a spherical region of interest (ROI) of approximately 4 mm around these cortical interruptions was identified for MCP joints and 2 mm for PIP joints. Fourth, voids in this ROI of ≥ 0.41 mm in radius were selected and only those connected to the cortical interruptions were included as underlying trabecular voids.

Per joint, the number, surface area and volume (cortical interruption and trabecular void volume) of the cortical interruptions were obtained (further described as "cortical interruption parameters").

Bone Density and Micro-structure Parameters

The standard evaluation protocol was used to determine the vBMD and micro-structural parameters as described elsewhere [23]. The vBMD (mgHA/cm^3) was calculated for the total (Tot.BMD), trabecular (Tb.BMD), and cortical (Ct.BMD) region. Furthermore, trabecular number (Tb.N) (mm^{-1}), thickness (Tb.Th) (μm), separation (Tb.Sp) (μm), and intra-individual distribution of separation (Tb.SpSD) (μm) were determined to assess the trabecular compartment. The cortical thickness (Ct.Th) (μm) was determined to assess the cortical compartment.

3D Image Registration

Joints were further qualitatively examined for bone repair and bone loss using 3D rigid image registration to exactly overlay the baseline and follow-up image. Each stack and each bone of the joint was registered separately to avoid registration errors due to stack shifts and different joint angles.

An overlay image was created by subtracting the follow-up from the baseline density image as described elsewhere [24].

Statistics

Descriptives per joint were calculated for cortical interruption-, vBMD-, and micro-structural parameters on HR-pQCT at baseline and 1-year follow-up. Within-group changes over time were tested with paired t test, between-group changes with independent t test.

Cumulative probability plots were made to evaluate changes at the individual joint level in the cortical interruption parameters and total BMD. Joints could show bone repair, progressive damage or no change over time according to the absolute least significant change (LSC$_{SD}$) cut-off values for the cortical interruption parameters obtained from previous research [21]. 'Repair' was defined as a decrease of at least 4 interruptions, 5.8 mm^2 in interruption surface area, or 3.2 mm^3 in interruption volume in a single joint, and 'progression' as an increase in these parameters, using the same cut-offs in the opposite direction [21]. The same was done with respect to the LSC$_{SD}$ cut-off value for bone density, which is a change of at least 10.6 mgHA/cm^3 in total BMD [21]. The proportion of joints showing either bone repair or progression was calculated for each of the cortical interruption parameters separately and proportions were compared using multivariable logistic regression with correction for baseline value and age, or by Fisher exact test in case of a proportion of 0%. Last, Pearson correlations between changes in cortical interruption parameters and changes in vBMD- and micro-structural parameters were calculated in each of the joints assessed.

Statistical analyses were performed using SPSS Version 20.0 (IBM Corp., Armonk, NY). For between-group comparisons, the significance level was set at 0.01 to correct for multiple testing. For all other analyses, a significance level of 0.05 was used.

Results

Seventy-nine subjects agreed to participate in the MOSA-hand cohort, but 13 subjects declined participation of the second visit (Supplemental Fig. 1). Fifty scans were excluded because of motion artefacts or a visible erosion on CR. In total, 32 patients with RA (221 scans) and 32 HS (116 scans) were included in the present study.

The patients had on average low disease activity and functional impairment (mean ESR 6.4 (7.7), mean HAQ 0.9 (0.6), Table 1). Seventeen (53%) patients were treated with bDMARDs. The patients had a significantly higher baseline SvdH hand score than HS.

Table 1 Characteristics of the participants

	Patients with RA $n = 32$	Healthy subjects $n = 32$	p-value
Age, years	53.9 (6.9)	51.4 (10.9)	0.225
Disease duration, months	129.2 (121.4)	n/a	
ESR	6.4 (7.7)	n/a	
HAQ	0.9 (0.6)	n/a	
ACPA positive	21 (66%)[b]	n/a	
RF positive	23 (72%)	n/a	
ACPA and RF positive	18 (56%)[b]	n/a	
Use of sDMARDs	28 (88%)	n/a	
Use of bDMARDs	17 (53%)[a]	n/a	
Use of sDMARDs and bDMARDs	13 (41%)[a]	n/a	
Smoking			
No	15 (47%)	19 (59%)	0.576
Former	11 (34%)	11 (34%)	
Current	6 (19%)	3 (9%)	
Baseline SvdH score	7.33 (12.39)	1.20 (1.92)[b]	< 0.001

All values are presented as mean (SD) or absolute number (%)

RA rheumatoid arthritis, *ESR* erythrocyte sedimentation rate, *HAQ* health assessment questionnaire, *ACPA* anti-citrullinated protein antibody, *RF* rheumatoid factor, *sDMARD* synthetic disease modifying anti-rheumatic drug, *bDMARD* biological disease modifying anti-rheumatic drug, *SvdH score* Sharp van der Heijde score, *SD* standard deviation, *n/a* not applicable

[a]One patient value is missing

[b]Two patient values are missing

Changes in Cortical Interruption Parameters

At baseline, significantly more cortical interruptions, a larger surface area and volume of cortical interruptions were detected in MCP, but not PIP joints, of patients with RA compared with HS (Table 2).

On the group level, the mean in cortical interruption parameters did not significantly change in patients with RA and HS. No between-group differences in mean change of the cortical interruption parameters were found.

Cumulative probability plots of the change in number, surface area, and volume of interruptions showed that repair and progression of cortical interruptions occurred in some joints, both in RA and HS (Fig. 1a). When applying the LSC_{SD} cut-off values, the proportion of joints showing repair in cortical interruptions was higher in patients with

Table 2 Values of the HR-pQCT cortical interruption parameters in MCP and PIP joints in patients with RA and healthy subjects

MCP joints	Patients with RA			Healthy subjects			p-value (change RA versus HS)
	Baseline $n = 107$	Follow-up $n = 107$	p-value	Baseline $n = 55$	Follow-up $n = 55$	p-value	
Number of interruptions	3.25 (3.97)*	2.93 (3.94)	0.144	1.45 (1.55)	1.64 (1.69)	0.345	0.084
Interruption surface area (mm^2)	5.89 (12.65)*	5.70 (12.87)	0.508	1.41 (2.00)	1.54 (2.39)	0.494	0.351
Interruption volume (mm^3)	13.92 (44.66)*	15.49 (58.17)	0.430	1.77 (6.10)	1.75 (6.09)	0.939	0.429
PIP joints	$n = 114$	$n = 114$		$n = 61$	$n = 61$		
Number of interruptions	1.60 (2.72)	1.89 (3.10)	0.037	0.92 (1.41)	0.87 (1.47)	0.684	0.063
Interruption surface area (mm²)	2.61 (7.10)	2.86 (6.79)	0.802	0.98 (1.80)	0.96 (1.76)	0.828	0.283
Interruption volume (mm³)	3.67 (15.82)	3.39 (13.05)	0.488	1.00 (3.35)	0.99 (2.57)	0.930	0.837

Values are displayed as mean (SD) per joint

RA rheumatoid arthritis, *HS* healthy subject, *MCP joint* metacarpophalangeal joint, *PIP joint* proximal interphalangeal joint, *HR-pQCT* high-resolution peripheral quantitative computed tomography, *SD* standard deviation

*$p < 0.01$, baseline RA versus HS

RA compared with HS for the number, surface area, and volume of interruptions (4.1%, 3.6%, and 6.6% versus 0%, 0%, and 1.7%, respectively), and this difference was significant for the volume of interruptions [Odd's ratio (OR) 6.6 (95% CI 1.08–39.9), $p = 0.041$]. The proportion of joints showing progression in cortical interruptions was not significantly different between the groups (4.1%, 2.7%, and 5.9% versus 0.9%, 0%, and 2.6%, respectively).

Typical examples of changes in cortical interruptions in MCP and PIP joints are shown in Figs. 2 and 3. Heterogeneous patterns of repair (Fig. 2) and progression (Fig. 3) of cortical interruptions can be seen. Repair of cortical interruptions was characterized by complete bridging of the cortical interruption with persisting trabecular bone void (Fig. 3a, b), complete filling of a small interruption (Fig. 3c), sclerosis within and around the trabecular bone void of the cortical interruption (Fig. 3c, d, respectively). Progression of cortical interruptions was characterized by the appearance of new cortical interruptions with and without underlying trabecular bone loss (Fig. 2a–e, black arrows), widening of a small cortical interruption (Fig. 2c, right black arrow), cortical thinning and increase in cortical porosity (Fig. 2a–e, blue arrows).

Changes in vBMD and Bone Micro-structural Parameters

At baseline, a significantly lower vBMD in the total, cortical and trabecular region was found in MCP and PIP joints of patients with RA compared with HS, except for Ct.BMD in PIP joints (Table 2). Furthermore, an impaired microstructure (Tb.N lower, and Tb.Sp and Tb.SpSD higher) was found in MCP and PIP joints of patients with RA compared with HS.

Table 3 shows that in both MCP and PIP joints, vBMD was decreased after 1 year in both patients with RA (range −3.3 to −5.9 mgHA/cm^3) and HS (range −1.1 to −3.3 mgHA/cm^3), and this decrease was significant for patients with RA. The decrease in total and trabecular vBMD in MCP joints was significantly more pronounced in patients with RA compared with HS (Table 3).

Cortical thickness also significantly decreased in both MCP and PIP joints in patients with RA after 1 year. In HS, only cortical thickness in MCP joints significantly decreased. Cumulative probability plots of total BMD show that most joints lose BMD and that this loss of BMD was more pronounced in patients with RA than in HS (Fig. 1a). The proportion of joints with loss in BMD beyond LSC was significantly higher in patients with RA than in HS (26.7% versus 12.9%, respectively, OR 2.6 (95% CI 1.4–5.0), $p = 0.004$, Fig. 1a). Increase in BMD beyond LSC was observed in 3.2% and 4.3% of the joints of patients with RA and HS, respectively.

Comparison of sDMARDs with bDMARDs

Figure 1b shows cumulative probability plots of patients treated with sDMARDs or bDMARDs. The proportion of joints showing repair in cortical interruptions was not significantly different between the groups for the number, surface area and volume of interruptions (3.0%, 2.0%, and 6.1% versus 5.3%, 5.3%, and 7.9%, respectively). The proportion of joints showing progression was significantly higher for the number of interruptions in patients on sDMARDs compared with bDMARDs (6.1% versus 1.8%, OR 6.6 (95% CI 1.0–41.7), $p = 0.048$), but not for the surface area and volume of interruptions (3.0% and 4.0% versus 1.8% and 7.9%, respectively).

The proportion of joints with loss in BMD beyond LSC was significantly higher in patients on sDMARDs compared with bDMARDs (31.3% versus 17.2%, respectively, OR 2.7 (95% CI 1.4–5.3), $p = 0.004$, Fig. 1b).

Changes in vBMD and bone micro-structural parameters were significantly correlated to changes in cortical interruption parameters of joints assessed in both patients with RA and HS (Supplemental Table 1).

Discussion

The present study showed that with semi-automatic HR-pQCT image analysis, cortical interruption-, vBMD- and micro-structural parameters were impaired in patients with RA compared with HS, of which vBMD and micro-structural parameters further deteriorated after 1 year. Furthermore, proportionally more joints of patients on sDMARDs showed progression in the number of interruptions and loss in vBMD compared with patients on bDMARDs.

As expected, cortical interruptions could be identified in both patients with RA and HS, but their number, surface area and volume were significantly greater in patients, and vBMD and bone micro-structure were also significantly impaired in patients with RA. These observations are in line with other studies [7, 13, 25–28]. At the group level, the mean in cortical interruption parameters did not change in patients with RA and HS over a 1-year period Interestingly, HS showed loss in total BMD, primarily caused by loss in cortical BMD and thinning of the cortical bone. This can be expected with aging [29]. Patients with RA additionally showed a significant decrease in trabecular BMD and trabecular thickness. Changes in vBMD and micro-structural parameters were correlated to changes in cortical interruption parameters, corresponding to observations from others [12].

In patients with RA, we showed heterogeneous patterns of changes indicating repair of cortical interruptions. Partial
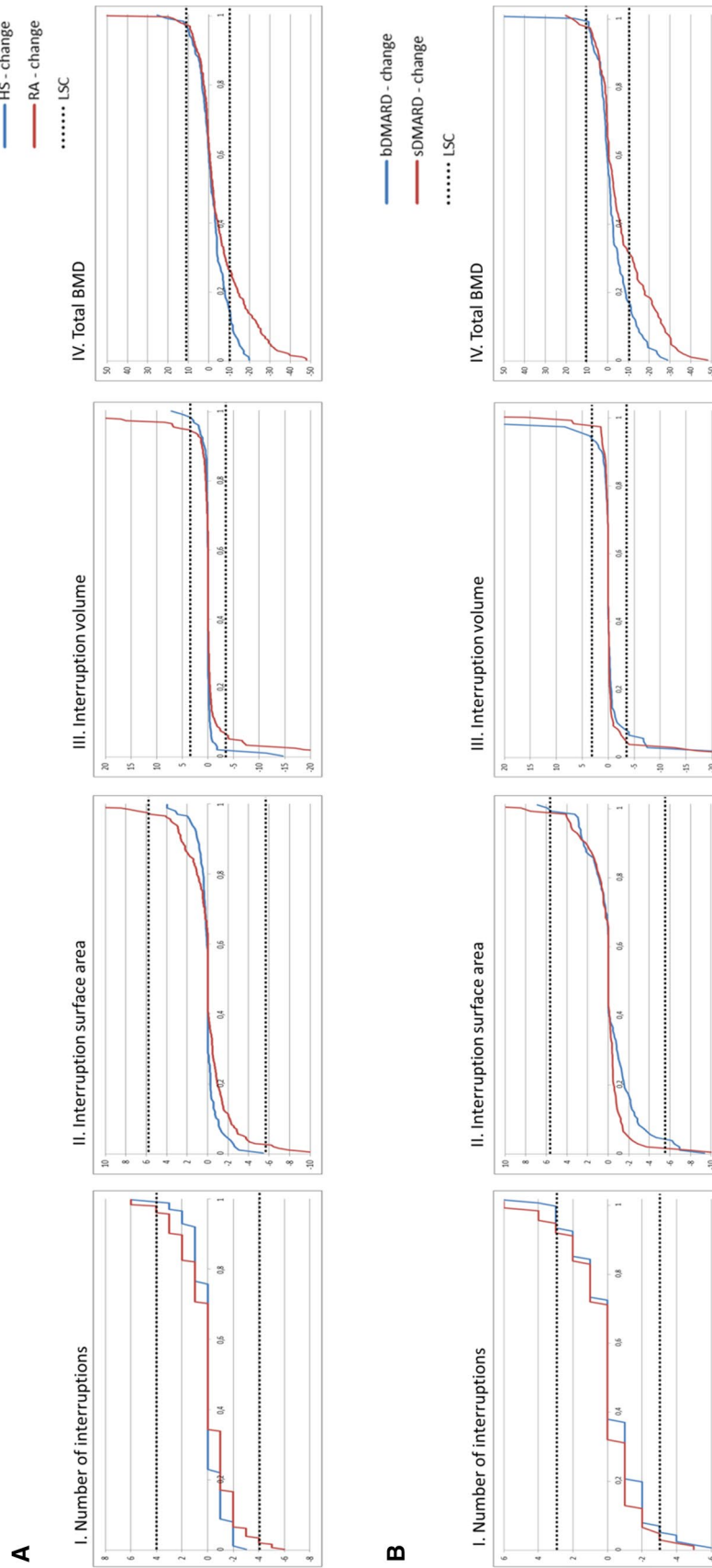
Fig. 1 Cumulative probability plots of changes in each joint of **a** individual patients with RA and healthy subjects, **b** patients on bDMARDs and sDMARDs. Plots of the change in the number, surface area, and volume of interruptions, and total BMD with corresponding LSC$_{SD}$ are displayed. (I–III) The plots show that more joints exceed the LSC$_{SD}$ threshold in both positive and negative direction in **a** patients with RA compared with healthy subjects, **b** sDMARDs compared with bDMARDs. Exceedance is approximately equally distributed in either direction for all cortical interruption parameters. (IV) Shows that the proportion of joints with significant loss of BMD was higher in **a** patients with RA compared with healthy subjects, **b** sDMARDs compared with bDMARDs. *RA* rheumatoid arthritis, *HS* healthy subject, *BMD* volumetric bone mineral density, *LSC* least significant change, *sDMARD* synthetic disease modifying anti-rheumatic drug, *bDMARD* biological DMARD
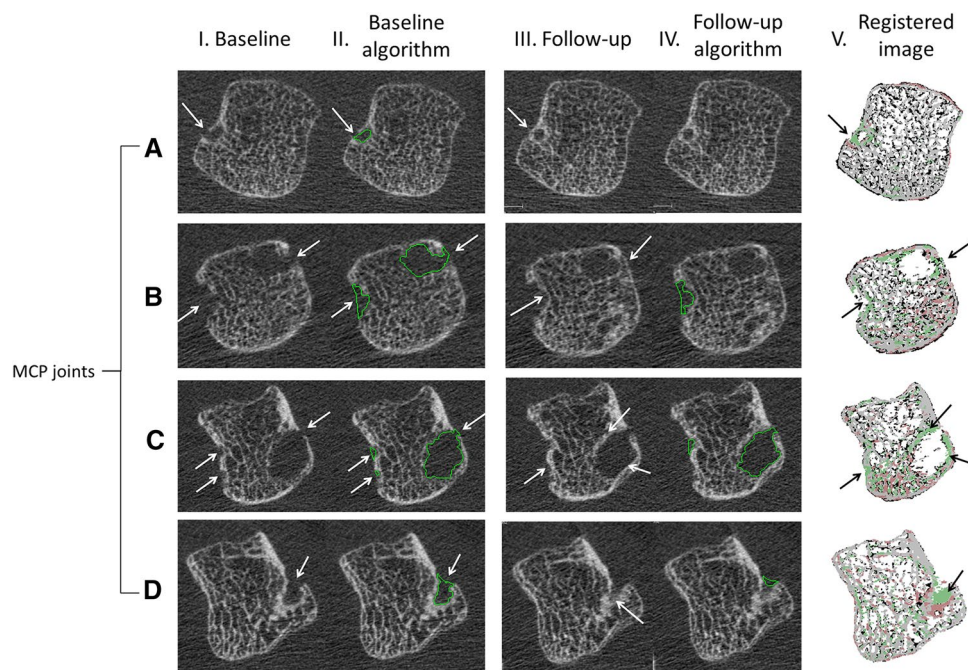
Fig. 2 Typical examples of bone repair in MCP joints (**a–d**) in patients with RA. (I) The baseline 2D slice with one or more cortical interruptions (white arrows). (II) Shows that the cortical interruptions are accurately detected by the algorithm at baseline (green circles). (III) Shows the corresponding follow-up image with the (partially) repaired cortical interruptions. (IV) Shows that most cortical interruptions are still detected by the algorithm (green circles), hence only partial repair of the cortical interruptions was observed in most cases. (V) Shows the 3D registered follow-up with baseline image, shown in green are the locations of bone repair, red bone loss and white no change, the black arrows indicate locations of bone repair in the cortical interruptions. Shown is that the locations of bone gain at the follow-up image match with the registered image (green color). (III-**a, b**) Shows bridging of the cortical bone, with persisting trabecular bone void. (III-**c, d**) Shows (partial) repair of the trabecular void volume, and complete filling of a small cortical interruption

repair of erosions in RA has been documented earlier using clinical standard imaging modalities (i.e., CR, MRI and clinical CT) [30–32]. Using HR-pQCT imaging, Töpfer et al. retrospectively and semi-automatically analyzed changes in volume and composition of surrounding bone of 40 erosions in patients with RA (45% treated with bDMARDs) over a mean follow-up of 1.2 years (11). Eight (20%) erosions decreased in volume beyond the LSC, with an increase of surrounding BMD suggestive for sclerosis, which is in accordance with our findings. They did, however, not detect complete bridging of cortical interruptions with persisting trabecular bone void or complete filling of a small cortical interruption, as we found.

We also showed heterogeneous patterns of changes indicating progression. In the study of Töpfer et al., six (15%) erosions showed progression in volume, with a decrease of surrounding BMD [11]. In contrast to our study, the investigators only analyzed existing erosions; no image analysis was performed to detect new erosions.

In our study, patients on sDMARDs showed more frequently progression in the number of interruptions per joint beyond LSC and more loss of total BMD compared with patients on bDMARDs. The effect of bDMARD treatment on repair of pathological interruptions detected on HR-pQCT has been described earlier [8, 9, 12]. Finzel et al. evaluated change in erosions in RA patients treated with Tumour Necrosis Factor alpha inhibitor (TNFi) compared with sDMARDs after 1 year. In patients on TNFi, a significant decrease in erosion depth (-0.1 mm) was found, characterized by sclerosis at the base of the erosion, but the width remained unchanged [8]. In contrast, in patients on sDMARDs, a significant increase in erosion depth and width was found, but no between-group comparison was performed. In another study by Finzel et al., Interleukin-6 receptor antibody treatment resulted in a decrease in mean erosion width (-0.1 mm), especially when sclerosis was present. However, also nine new erosions were detected at the 1-year follow-up [9]. In this study, no comparison was made to an sDMARD treatment group. Shimizu et al. reported change in both erosion volume and vBMD in RA patients treated with TNFi compared with sDMARDs after 3 months [12]. A significant decrease in erosion volume (-3.8 mm^3) was found in patients on TNFi, and an increase in volume ($+0.9$ mm^3) in patients on sDMARDs. No new erosions were detected [12]. Although they did not find a mean change in vBMD, they observed that changes in vBMD significantly correlated with changes in erosion volume. These studies were done in single, visually identified, erosions [8, 9, 12]. In contrast
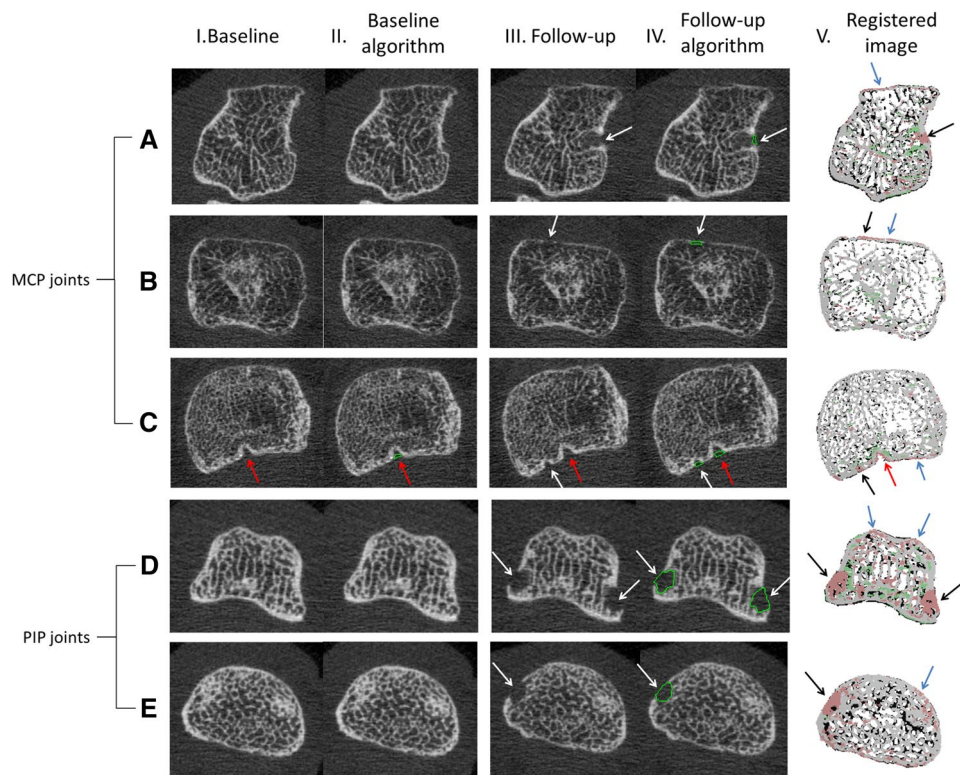
Fig. 3 Typical examples of new incident cortical interruptions and bone loss in MCP (**a**–**c**) and PIP (**d**, **e**) joints of patients with RA (**b**–**e**) and healthy subjects (**a**). (I) Shows a baseline 2D slice, and (II) shows that the algorithm detected the cortical interruption accurately. (III) Shows the corresponding follow-up image with the new incident cortical interruptions (white arrows). (III) Shows that the new incident cortical interruptions are accurately detected by the algorithm (green circles). (IV) Shows the overlayed images, in green are the locations of bone gain, in red bone loss and in white no change, the arrows indicate locations of bone loss. Shown is that indeed at locations of bone loss (red color) new interruptions are detected at follow-up. (IV-**a, c**–**e**) Show examples of new cortical interruptions with and without underlying trabecular bone loss (black arrows), and cortical bone loss (blue arrows) (IV-**b**) Shows an example of cortical thinning leading to a cortical interruption, (IV-**c**) Shows an example of widening of a small cortical interruption

to our study, small cortical interruptions and bone microstructure were not evaluated in these studies.

The strengths of our study are the prospective design of the study, inclusion of patients with RA and HS, and the application of fully automatic detection of cortical interruptions, after contouring of the bone, which makes it user-friendly and avoids intra- and inter-reader variability [5]. Our study has several limitations. First, this is an observational study and hence confounding by indication might give bias in the comparison of patients treated with bDMARDs versus sDMARDs. Second, although we had information on ESR, we did not assess disease activity with the generally accepted disease activity score with 28 joints (DAS-28) [33] in patients with RA, because this information was lacking in many patients. Therefore, we could not assess its influence on bone loss. Furthermore, 12.8% of the joints had to be excluded due to motion

artefacts. Possibly, motion artefacts occur more frequently in a subgroup of patients with RA, for example in patients with more severe RA or elderly, introducing bias.

In conclusion, the present study showed that HR-pQCT is able to quantify bone repair and loss in finger joints in RA and HS. Cortical interruption-, vBMD-, and microstructural parameters were impaired in patients with RA compared with HS, of which vBMD and micro-structural parameters further deteriorated. Furthermore, in patients on sDMARDs, significantly more decrease in vBMD compared with patients on bDMARDs was found. HR-pQCT with our semi-automated algorithm showed promising results for monitoring treatment effects in RA.

Table 3 HR-pQCT bone density, and micro-structure parameters in MCP joints of healthy subjects and patients with RA

MCP joints	Patients with RA				Healthy subjects				p-value (change RA versus HS)
	Baseline n = 107	Follow-up n = 107	Mean change	p-value	Baseline n = 55	Follow-up n = 55	Mean change	p-value	
Bone density parameters									
Tot.BMD (mg HA/cm^3)	292.1 (50.1)*	287.7 (49.8)	−4.4	<0.001	321.6 (36.0)	320.5 (36.2)	−1.1	0.030	0.002
Tb.BMD (mg HA/cm^3)	187.7 (35.5)*	184.4 (35.9)	−3.3	<0.001	206.3 (20.2)	205.7 (19.8)	−0.6	0.219	0.001
Ct.BMD (mg HA/cm^3)	628.0 (66.2)*	622.1 (66.5)	−5.9	<0.001	664.1 (53.6)	661.5 (55.7)	−2.6	0.018	0.081
Bone micro-structure parameters									
Tb.N (mm^{-1})	1.57 (0.43)*	1.58 (0.44)	+0.01	0.533	1.77 (0.31)	1.78 (0.29)	+0.01	0.882	0.827
Tb.Th (µm)	102.9 (16.8)	101.1 (18.0)	−1.8	0.012	98.9 (13.6)	98.3 (13.4)	−0.6	0.503	0.286
Tb.Sp (µm)	586.1 (198.5)*	588.8 (207.8)	+2.7	0.584	483.9 (100.3)	482.0 (96.4)	−1.9	0.674	0.540
Tb.SpSD (µm)	691.3 (380.3)*	679.8 (393.9)	−11.5	0.214	480.3 (264.0)	473.2 (258.5)	−7.1	0.520	0.750
Ct.Th (µm)	351.5 (108.5)	342.6 (110.2)	−8.9	0.001	411.6 (108.4)	406.2 (111.4)	−5.4	0.002	0.355
PIP joints	n = 114	n = 114			n = 61	n = 61			
Bone density parameters									
Tot.BMD (mg HA/cm^3)	468.7 (68.8)*	462.9 (66.3)	−5.8	<0.001	504.9 (54.7)	502.3 (56.9)	−2.6	0.046	0.079
Tb.BMD (mg HA/cm^3)	274.2 (36.3)*	272.5 (35.9)	−1.7	<0.001	292.2 (22.8)	291.3 (22.4)	−0.9	0.101	0.157
Ct.BMD (mg HA/cm^3)	703.8 (65.8)*	697.9 (61.4)	−5.9	<0.001	731.8 (54.3)	728.5 (57.7)	−3.3	0.028	0.252
Bone micro-structure parameters									
Tb.N (mm^{-1})	1.82 (0.29)*	1.83 (0.30)	+0.01	0.417	1.95 (25.5)	1.93 (25.7)	−0.02	0.069	0.043
Tb.Th (µm)	127.0 (14.8)	125.6 (14.7)	−1.4	0.033	126.0 (23.5)	127.3 (12.9)	+1.3	0.151	0.015
Tb.Sp (µm)	437.7 (91.4)*	436.2 (90.7)	−1.5	0.687	394.6 (59.8)	400.5 (60.2)	+5.9	0.062	0.084
Tb.SpSD (µm)	366.3 (148.1)*	362.3 (152.1)	−4.0	0.471	284.9 (116.3)	283.4 (110.6)	−1.5	0.768	0.777
Ct.Th (µm)	588.9 (184.1)	575.3 (177.7)	−13.6	<0.001	666.1 (166.2)	659.8 (171.8)	−6.3	0.093	0.139

Values are displayed as mean (SD)

RA rheumatoid arthritis, *HS* healthy subject, *MCP joint* metacarpophalangeal joint, *HR-pQCT* high-resolution peripheral quantitative computed tomography, *BMD* bone mineral density, *Tot.BMD* total volumetric BMD, *Tb.BMD* trabecular volumetric BMD, *Ct.BMD* cortical volumetric BMD, *Tb.N* trabecular number, *Tb.Th* trabecular thickness, *Tb.Sp* trabecular separation, *Tb.SpSD* intra-individual trabecular separation, *Ct.Th* cortical thickness, *SD* standard deviation, *HA* hydroxyapatite

*$p < 0.01$, baseline RA versus HS

Compliance with Ethical Standards

References

1. Schett G, Gravallese E (2012) Bone erosion in rheumatoid arthritis: mechanisms, diagnosis and treatment. Nat Rev Rheumatol 8(11):656–664
2. Geusens P, van den Bergh J (2014) Bone erosions in rheumatoid arthritis. Rheumatology 53(1):4–5
3. Burghardt AJ, Link TM, Majumdar S (2011) High-resolution computed tomography for clinical imaging of bone microarchitecture. Clin Orthop Relat Res 469(8):2179–2193
4. Lee CH, Srikhum W, Burghardt AJ, Virayavanich W, Imboden JB, Link TM et al (2015) Correlation of structural abnormalities of the wrist and metacarpophalangeal joints evaluated by high-resolution peripheral quantitative computed tomography, 3 T magnetic resonance imaging and conventional radiographs in rheumatoid arthritis. Int J Rheum Dis 18(6):628–639
5. Peters M, Scharmga A, de Jong J, van Tubergen A, Geusens P, Arts JJ et al (2017) An automated algorithm for the detection of cortical interruptions on high resolution peripheral quantitative computed tomography images of finger joints. PLoS ONE 12(4):e0175829
6. Scharmga A, Peters M, van Tubergen A, van den Bergh J, Barnabe C, Finzel S et al (2016) Heterogeneity of cortical breaks in hand joints of patients with rheumatoid arthritis and healthy controls imaged by High-resolution peripheral quantitative computed tomography. J Rheumatol 43(10):1914–1920
7. Fouque-Aubert A, Boutroy S, Marotte H, Vilayphiou N, Bacchetta J, Miossec P et al (2010) Assessment of hand bone loss in rheumatoid arthritis by high-resolution peripheral quantitative CT. Ann Rheum Dis 69(9):1671–1676
8. Finzel S, Rech J, Schmidt S, Engelke K, Englbrecht M, Stach C et al (2011) Repair of bone erosions in rheumatoid arthritis treated with tumour necrosis factor inhibitors is based on bone apposition at the base of the erosion. Ann Rheum Dis 70(9):1587–1593
9. Finzel S, Rech J, Schmidt S, Engelke K, Englbrecht M, Schett G (2013) Interleukin-6 receptor blockade induces limited repair of bone erosions in rheumatoid arthritis: a micro CT study. Ann Rheum Dis 72(3):396–400
10. Yue J, Griffith JF, Xiao F, Shi L, Wang D, Shen J et al. (2016) Repair of bone erosion in rheumatoid arthritis by denosumab: a high-resolution peripheral quantitative computed tomography study. Arthritis Care Res 69:1156–1163
11. Topfer D, Gerner B, Finzel S, Kraus S, Museyko O, Schett G et al. (2015) Automated three-dimensional registration of high-resolution peripheral quantitative computed tomography data to quantify size and shape changes of arthritic bone erosions. Rheumatology 54:2171–2180
12. Shimizu T, Choi HJ, Heilmeier U, Tanaka M, Burghardt AJ, Gong J et al (2017) Assessment of 3-month changes in bone microstructure under anti-TNFalpha therapy in patients with rheumatoid arthritis using high-resolution peripheral quantitative computed tomography (HR-pQCT). Arthritis Res Ther 19(1):222
13. Stach CM, Bauerle M, Englbrecht M, Kronke G, Engelke K, Manger B et al (2010) Periarticular bone structure in rheumatoid arthritis patients and healthy individuals assessed by high-resolution computed tomography. Arthritis Rheum 62(2):330–339
14. Peters M, Scharmga A, van Tubergen A, Arts J, Loeffen D, Weijers R et al (2017) The reliability of a semi-automated algorithm for detection of cortical interruptions in finger joints on high resolution CT compared to MicroCT. Calcif Tissue Int 101:132–140
15. Aletaha D, Neogi T, Silman AJ, Funovits J, Felson DT, Bingham CO et al (2010) 2010 Rheumatoid arthritis classification criteria: an American College of Rheumatology/European league against rheumatism collaborative initiative. Arthritis Rheum 62(9):2569–2581
16. Bruce B, Fries JF (2003) The Stanford Health Assessment Questionnaire: dimensions and practical applications. Health Qual Life Outcomes 1:20
17. van der Heijde D (1999) How to read radiographs according to the Sharp/van der Heijde method. J Rheumatol 26(3):743–745
18. Barnabe C, Feehan L, Spectra (2012) High-resolution peripheral quantitative computed tomography imaging protocol for metacarpophalangeal joints in inflammatory arthritis: the SPECTRA collaboration. J Rheumatol 39(7):1494–1495
19. Barnabe C, Szabo E, Martin L, Boyd SK, Barr SG (2013) Quantification of small joint space width, periarticular bone microstructure and erosions using high-resolution peripheral quantitative computed tomography in rheumatoid arthritis. Clin Exp Rheumatol 31(2):243–250
20. Pialat JB, Burghardt AJ, Sode M, Link TM, Majumdar S (2012) Visual grading of motion induced image degradation in high resolution peripheral computed tomography: impact of image quality on measures of bone density and micro-architecture. Bone 50(1):111–118
21. Peters M, de Jong J, Scharmga A, van Tubergen A, Geusens P, Loeffen D et al (2018) An automated algorithm for the detection of cortical interruptions and its underlying loss of trabecular bone; a reproducibility study. BMC Med Imaging 18(1):13
22. Laib A, Hauselmann HJ, Ruegsegger P (1998) In vivo high resolution 3D-QCT of the human forearm. Technol Health Care 6(5–6):329–337
23. Boutroy S, Bouxsein ML, Munoz F, Delmas PD (2005) In vivo assessment of trabecular bone microarchitecture by high-resolution peripheral quantitative computed tomography. J Clin Endocrinol Metab 90(12):6508–6515
24. Christen P, Boutroy S, Ellouz R, Chapurlat R, van Rietbergen B (2018) Least-detectable and age-related local in vivo bone remodelling assessed by time-lapse HR-pQCT. PLoS ONE 13(1):e0191369
25. Simon D, Kleyer A, Stemmler F, Simon C, Berlin A, Hueber AJ et al (2017) Age- and sex-dependent changes of intra-articular cortical and trabecular bone structure and the effects of rheumatoid arthritis. J Bone Miner Res 32(4):722–730
26. Yang H, Yu A, Burghardt AJ, Virayavanich W, Link TM, Imboden JB et al (2015) Quantitative characterization of metacarpal and radial bone in rheumatoid arthritis using high resolution-peripheral quantitative computed tomography. Int J Rheum Dis 20:353–362
27. Werner D, Simon D, Englbrecht M, Stemmler F, Simon C, Berlin A et al (2017) Rheumatoid arthritis is characterized by early changes of the cortical micro-channel (CoMiC) system in the bare area of the joints. Arthritis Rheum 69:1580–1587
28. Peters M, van Tubergen A, Scharmga A, Driessen A, van Rietbergen B, Loeffen D et al (2018) Assessment of cortical interruptions in the finger joints of patients with rheumatoid arthritis using HR-pQCT, radiography, and MRI. J Bone Miner Res 33(9):1676–1685

29. Feehan LM, Li LL, McKay HA (2017) Micro-structural bone changes in early rheumatoid arthritis persist over 1-year despite use of disease modifying anti-rheumatic drug therapy. BMC Musculoskelet Disord 18(1):521

30. Ideguchi H, Ohno S, Hattori H, Senuma A, Ishigatsubo Y (2006) Bone erosions in rheumatoid arthritis can be repaired through reduction in disease activity with conventional disease-modifying antirheumatic drugs. Arthritis Res Ther 8(3):R76

31. van der Linden MP, Boja R, Klarenbeek NB, Huizinga TW, van der Heijde DM, van der, Helm-van Mil AH (2010) Repair of joint erosions in rheumatoid arthritis: prevalence and patient characteristics in a large inception cohort. Ann Rheum Dis 69(4):727–729

32. Dohn UM, Ejbjerg B, Boonen A, Hetland ML, Hansen MS, Knudsen LS et al (2011) No overall progression and occasional repair of erosions despite persistent inflammation in adalimumab-treated rheumatoid arthritis patients: results from a longitudinal comparative MRI, ultrasonography, CT and radiography study. Ann Rheum Dis 70(2):252–258

33. Prevoo ML, van't Hof MA, Kuper HH, van Leeuwen MA, van de Putte LB, van Riel PL (1995) Modified disease activity scores that include twenty-eight-joint counts. Development and validation in a prospective longitudinal study of patients with rheumatoid arthritis. Arthritis Rheum 38(1):44–48